



An experimental study of the behaviour of sandwich composite panels under low-speed loading

Opukuro David-West¹  and Anish Girish Advani¹

Abstract

While natural fibres may not match the mechanical properties of synthetics ones, they offer the environmental benefits. Hybridisation is one approach to enhance the mechanical performance for relatively moderate strength applications. In this investigation, the characteristics of sandwich composites with carbon fibre reinforced laminates as the skin structure with core materials of hemp fibre, Nomex honeycomb, and 3D Core infusion foam under quasi-static loading have been investigated and compared with the response of plate using flax fibre reinforcement for the skin laminate and the core materials remains the same. The samples were manufactured by hand layup and autoclave curing for the skin laminate and then glued to the core material. They were conducted using the universal testing machine at the loading rate of 10 mm/min. Two different fibre orientations, $[0^\circ/30^\circ/60^\circ/90^\circ]_s$ and $[0^\circ/\pm 45^\circ/90^\circ]_s$ were evaluated. The data collected from the tests were utilised to obtain the maximum load bearing capacity and energy absorbed by the samples. Additionally, the failure modes for all the samples were observed. Results indicate that panels with hemp fibre core exhibit superior mechanical properties compared to the other core materials, though with a rise in the weight. Samples with honeycomb and foam core demonstrated similar mechanical performance. Furthermore, the study reveals that different core materials are compatible with specific stacking sequences based on the material of the fibre reinforcement and that the spiral arrangement of $[0^\circ/30^\circ/60^\circ/90^\circ]_s$ is a recommendation to consider for improving damage resistance.

Keywords

sandwich composite, failure modes, peak load, energy absorbed, penetration test

Introduction

Materials are integral part of our society and daily lives. They play a significant role in defining the performance, durability, and functionality of manufactured products and structures. In recent years, carbon fibre-reinforced polymer composites (CFRPs) have gained significant attraction in some of the industrial application including the aerospace industry.¹ The aircraft manufacturers, like Boeing and Airbus, emphasised the use of CFRPs for secondary aircraft structures that do not compromise flight safety. About 30%–40% of modern airframes are now composed of composites, with this percentage steadily rising owing to ongoing technological advancements in the field.² This surge is primarily attributed to the impressive mechanical characteristics of fibre reinforce composites, which include low density, high tensile strength, and high modulus.

The samples used in this investigation were sandwich composite panels consisting of fibre reinforced composite skin of different configurations and different types

of core materials. The primary objective in manufacturing sandwich structures was to achieve optimal stiffness and strength while minimising the overall weight, which is attributed to the core structure. These kinds of structures are used by several industries including the civil, marine and aviation industries. Composite sandwich structures are lightweight, strong and termite resistant making them favourable for civil construction. They are also accepted in flooring systems because of the lightweight and strength properties, as with the reduction in weight smaller supporting

¹Centre for Engineering Research, Materials and Structures Group, University of Hertfordshire, Hatfield, UK

Corresponding author:

Opukuro David-West, Centre for Engineering Research, Materials and Structures Group, University of Hertfordshire, Hatfield AL10 9AB, UK.
 Email: o.david-west@herts.ac.uk

Data Availability Statement included at the end of the article.

members can be used. Sandwich composite panels with honeycomb core materials are widely used in the aerospace sector because of the stiffness-to-weight and strength-to-weight efficiencies and hence savings on the fuel consumption.

Research was conducted by Sadeghian et al.³ on sandwich composite beams manufactured with flax fibres reinforced polymer and glass fibre reinforced laminate as the skin material. Their findings indicated that sandwich composites featuring flax fibre reinforced polymer skin and natural cork core materials showed a comparable structural performance with respect to their counterparts made of glass fibre reinforced polymer skin and synthetic honeycomb core materials. Islam and Aravinthan⁴ tested sandwich composite panels made of glass fibre reinforced polymer skins and phenolic core material under point loading and distributed loading separately. The samples were supported at two edges and then on the four edges. They observed that the results were similar in both loading conditions. In addition, Malcon et al.⁵ reported about the compression characteristics of composite sandwich structures made of corrugated core with foam inserts and woven glass z-yarn fibres infused with epoxy skin.

Jin et al.⁶ tested sandwich structures with new integrated woven corrugated cores under compression, shear and bending loads to study the failure modes and mechanical properties; and observed that because of the anisotropic characteristics of the core the resistance to shear was improved. Also, Zhang et al.⁷ created corrugated sandwich composite structures and investigated on how to improve strength and stiffness by controlling the parameters of types of fibres, corrugation angle, core thickness and the bonding between the core the skin. They observed that hybridised glass fibres and carbon fibres (50:50) of the skin showed the same equivalent specific bending strength as that of carbon fibre composites only; also increase in the corrugation angles and thickness of the core enhanced the specific bending strength.

Furthermore, Hou et al.⁸ manufactured sandwich panels made of aluminium skin and trapezoidal aluminium cores and tested under crushing load. The core configurations of the samples varied as regular-arranged, stagger-arranged and cross-arranged (0/90). Their results revealed that the cross-arranged (0/90) panels performed better for the peak load and the energy absorbed. Then, Ruan et al.⁹ subject sandwich panels made of aluminium foam core and aluminium skin to static loading and concluded from the results obtained that thick face sheet structures resulted in higher load levels and peak load. In another related study Farrokhbadi et al.¹⁰ concluded that multilayer sandwich composite structures improved the strength and energy absorption significantly.

Sayahlatifi et al.¹¹ tested hybrid composite made of aluminium as the face sheet and the combination of balsa wood with E-glass fabric as the core under four points

bending load and found the behaviour suitable to avoid catastrophic failure. While Mahmoudabadi and Sadighi¹² conducted quasi-static punch test on sandwich panels of honeycomb metallic core and aluminium plate face sheet. Some failure modes such as face sheet wrinkling, debonding, tearing, core crushing were noted and concluded that increase in the thickness of the core improves the energy absorbed compared to increase of the skin thickness. Fan et al.¹³ in their study on quasi-static compression and three-point-bending tests on the woven textile sandwich material discussed about the failure mechanism of the structure.

Jackson and Shukla¹⁴ reported that high velocity impact on sandwich composite structures has the most effect on the exit face sheet compared to the core and impact face, while damage effect by low energy impact concentrated on the impact face sheet the side of the core attached to it. Chen et al.¹⁵ have developed a numerical model to interpret the damage characteristics of carbon fibre composite sandwich structures with honeycomb core subjected to impact loading and the finding were validated by comparison with the experimental data. In addition, Zhang et al.¹⁶ performed quasi-static loading test on sandwich composite beam made of carbon fibre-reinforced plastic skin and aluminium foam core to examine the failure characteristics and observed face-sheet fracture, indentation and core shear.

Hachemane et al.¹⁷ manufactured sandwich panels made of natural cork materials available in Algeria and jute/epoxy composite skin and tested them for impact loading and indentation to study the damage characteristics. The cork density and impact energy were key parameters influencing the maximum force and damage level. In another related study, Zhao et al.¹⁸ performed static loading test on pyramidal lattice stitched foam sandwich composite and compared the results to that obtained from foam sandwich structure and found significant improvement on the mechanical properties using the lattice stitched foam. In the study conducted by Mazzuca¹⁹ it was revealed that homogeneous polyethylene terephthalate (PET) sandwich panels demonstrate higher ultimate loads compared to their counterparts using polyurethane (PUR) foam, which was attributed to the superior shear strength of PET foam in contrast to PUR foam.

This study is about the characteristics of flat plate sandwich composite structures under quasi-static loading using flax fibre reinforce polymer and carbon fibre reinforced laminates as the skin structure with various forms of core materials (i.e., hemp fibre, honeycomb core, and recycled PET foam). The effect of various skins laminates of various stacking sequence was considered. Strength parameters extracted from the test data were compared to evaluate the effect of the core materials on the characteristics obtained from the composites under the low-speed loading. In addition, the structures with flax as part of the skin

Table 1. Overview of materials procured from easy composites.

Product Name	Product Description	Application
XC130 150 g unidirectional prepreg carbon fibre (300 mm)	Unidirectional prepreg carbon fibre weighing 150 gsm	Carbon fibre skin laminate
FLAXPREG 110 g unidirectional prepreg flax fibre (600 mm)	Unidirectional prepreg flax fibre weighing 110 gsm	Flax fibre skin laminate
150 g non-woven hemp fibre mat (480 mm)	Non-woven hemp mat weighing 110 gsm	Core material for sandwich panels
3.2 mm cell 29 kg Nomex aerospace honeycomb	'Aerospace Grade' Nomex [®] aramid paper honeycomb weighing 29 kg/m ³	Core material for sandwich panels
3DCORE PET 100 infusion foam	PET (polyethylene terephthalate) foam by 3D CORE [®]	Core material for sandwich panels

material makes them less expensive than synthetic fibres due to their abundance and renewability.

Materials selection

The materials were sourced from Easy Composites Ltd; a company well recognised for the production and distribution of advanced composite materials and equipment. Table 1 offers a summary of the materials employed in fabricating the composite sandwich panels used for this study.

The unidirectional Prepreg Carbon Fibre material is uncured and can be adopted to implement possible directional strength optimisation in the laminate production. The good mechanical performance of this material and quality appearance has made it useful in some of the structures in aerospace, wind energy, motorsports etc. The unidirectional Prepreg flax fibre is pre-impregnated with 50% epoxy resin by weight. It can serve as the recommended substitute for glass fibres in the design of composite structures for moderate load applications, limited environmental footprint, and cost. In Table 2 is presented the typical mechanical properties of carbon/epoxy lamina and flax/epoxy lamina.

The next material involved in the production of the composite panels used in this study is hemp, which is environmentally friendly and sustainable alternative to synthetic fibres such as glass but with consideration to the

loading involved. It is also a good choice for damping vibrations and absorbing sound.^{23,24} Another kind of core material used was the Nomex honeycomb with the density of 29 kg/m³ and it is very light. It is accepted for light weight applications like for the cabinets and lockers of aircrafts, racing vehicles etc. The third type of core material adopted in the fabrication of the structures tested was 3DCORE PET 100 Infusion Foam, produced as pattern of interconnected hexagons with a material density of 95 kg/m³. The strength properties of the infusion foam, hemp fibres and Nomex honeycomb as obtained from the manufacturer's data sheet are shown in Tables 3 and 4.

Structural design of composite is intended to meet specific requirements. The materials selected for the manufacture of the sandwich panels of various configurations in this investigation are used in the industries. The results about the damage management and characteristics of these engineered structures are to serve as pointers for the user of composites.

Manufacture of panel face sheet laminates and the configurations

The face sheet laminates of the sandwich panels were composites, some of carbon reinforced materials and others

Table 2. Typical mechanical properties of unidirectional carbon/epoxy ply²⁰ and flax/epoxy ply.^{21,22}

Parameter	Carbon/epoxy ply	Flax/epoxy ply
Longitudinal modulus, E_{11} (GPa)	235	31.42
Transverse modulus, E_{22} (GPa)	17	5.58
Transverse modulus, E_{33} (GPa)	17	5.58
Poisson's ratio, $\nu_{12} = \nu_{31}$	0.32	0.353
Shear moduli, $G_{12} = G_{23} = G_{13}$ (GPa)	4.5	2.07
Longitudinal tensile strength, X_1 (MPa)	3900	287.7
Longitudinal compressive strength, X_2 (MPa)	2400	127.1
Transverse tensile strength, Y_1 (MPa)	111	33.86
Transverse compressive strength, Y_2 (MPa)	290	79.94
In-plane shear strength, S (MPa)	50	37.35

Table 3. Properties of hemp fibre mat²⁵ and infusion foam.²⁶

Parameters	Infusion foam	Hemp fibre mat
Tensile strength (MPa)	1.44	108 ± 7
Tensile modulus (GPa)	7.71	11 ± 1
Compressive strength (MPa)	8.23	
Compressive modulus (GPa)	3.16	

of flax reinforced materials. They are products from Easy Composites Limited, and the material data sheet recommended the cure temperature between 120°C and 130°C. Using angle metallic plates and sharp blade composite plies were cut from the roll of fibre unidirectional epoxy matrix tape and stacked according to the stacking sequence shown in Table 5 by hand. The laminates were of the dimensions of 300 mm by 200 mm and then cut to 150 mm by 100 mm to get four samples from same configuration. The ply thicknesses were 0.3 mm and 0.22 mm for the carbon and flax products respectively. This dimension is for standardisation in accordance with of ASTM-D7136²⁸ test standard for impact and it was the available support fixture in the laboratory.

The laminates were cured with the autoclave product of vacuum furnace engineering (VFE) to attain the structural strength before combined with the core material to form the sandwich structure. The process applies the combination of pressure and vacuum on the samples. The vacuum tries to eliminate air in the bagging and entrapped within the plies during the layup, while the pressure helps to suppress vapour within the resin and prevent voids. In Figure 1 is the photograph of the autoclave with the samples bagged and placed on the bed of the autoclave and the bagging of the samples illustrated with schematic diagram of Figure 2.

The cycle used to produce laminates is illustrated in Figure 3. It was heated gradually from room temperature to 123°C at the rate of 1.5°C/min and maintained at this temperature for a period of 60 min. After which it was cooled at the rate of 5°C/min to 70°C and 50°C; held at these temperatures for 2 min and then allowed to cool gradually to room temperature. The samples were under a pressure of 4.14 bar during the process. After completion of the curing process in the autoclave, the assembly was carefully taken out of the unit; the sealant and bagging material removed, followed by the breather cloth and release film before taking

Table 4. Properties of Nomex honeycomb.²⁷

Parameters	Value
Compressive strength (stabilised)	0.9 MPa
Plate shear strength (lengthways)	0.5 MPa
Plate shear strength (widthways)	0.35 MPa
Plate shear modulus (widthways)	17 MPa
Plate shear modulus (lengthways)	25 MPa

Table 5. Stacking of face sheet laminates.

Ply material	Laminate configuration
Unidirectional carbon fibre epoxy	[0°/30°/60°/90°] _s
Unidirectional flax fibre epoxy	[0°/30°/60°/90°] _s
Unidirectional flax fibre epoxy	[0°/±45°/90°] _s
Unidirectional carbon fibre epoxy	[0°/±45°/90°] _s

it out. The removal of subsidiary material and cutting of the samples with a guillotine was carried out with great care to maintain test coupons quality.

Fabrication of the sandwich panels

The sandwich panels consisted of three layers, that is top face-sheet, core material and bottom face-sheet. For the fabrication of sandwich panels, the core material was affixed between the skin laminates using thin film of epoxy resin mixed with the hardener in a ratio of 3:1 following the manufacturer's specifications. The assembly was subjected to compression under weights and allowed to cure at room temperature for a duration of 48 h.

The process initiates with the preparation of the core material. Each core material was cut into standardised sizes of 100 mm by 150 mm, mirroring the dimensions of the skin samples. During fabrication, a single layer of PET foam or Nomex honeycomb was applied for each sample, while three layers of unwoven hemp fibres were employed for sandwich composites with hemp fibres as the core material. This decision was made because the hemp fibre layers were relatively thin, and increasing the number of layers was anticipated to enhance the performance of the composite. The non-woven hemp fibre mat product has the thickness of 0.29 mm and with the use of three layers stacked together makes the core thickness 0.87 mm. The Nomex honeycomb and PET infusion foam were of the same thickness of 3 mm. Sufficient volume of the resin was used to ensure the thorough wetting of the hemp fibres. In Figure 4 is the representative image of the manufactured test coupons.

Test set-up and procedure

The most frequently conducted mechanical tests on sandwich composites are measurements of compressive strength, three-point bending test, and impact tests.²⁹ Quasi-static loading or penetration tests, falling under the category of compressive strength measurements and are pivotal in analysing the mechanical behaviour of sandwich composite panels.

To conduct this test on the fabricated samples, a Tinius Olsen universal testing machine (UTM) equipped with an indenter, as illustrated in Figure 5 was utilised. A standard 12 mm diameter indenter was employed to ensure uniform

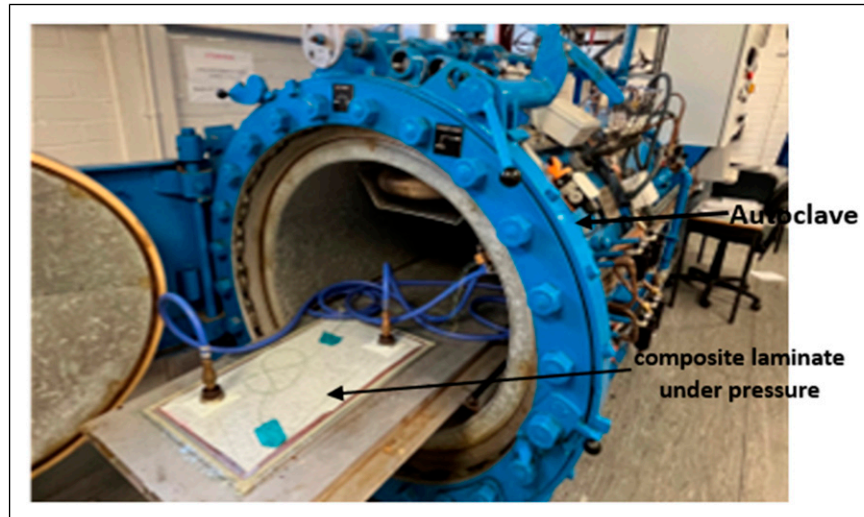


Figure 1. Autoclave loaded with laminate for curing.

distribution of the load exerted by the machine. To secure the sample in place during the test and prevent any movement, a dedicated test rig, depicted in Figure 6 was employed. This rig provided stability and ensured consistent testing conditions throughout the duration of the experiment. For safety precautions, a protective shield was positioned in front of the test section to shield against any potential debris ejected during the experiment.

The test rig comprised of a baseplate for supporting the test sample, featuring a central rectangular aperture. On top of the test sample is a fixture with rectangular hole held by four pressure plates applied through screw bolts. Additionally, the test rig has extra toggle clamps. Before testing, the thickness of each sample was measured using a digital vernier calliper. Five readings were taken at different locations on the surface, and the average value was calculated. Subsequently, the indenter was gently lowered closer to the surface of the sample, and it was ensured that the indenter was centrally aligned with the sample.

The test machine has a maximum loading capacity of 25 kN and the samples were loaded at a crosshead speed

of 10 mm/min. During the test the resistive force exerted by the sample on the indenter is detected by the load cell and is measured as a function the displacement of the loading point. The indenter was loaded on the sample till penetration. The complete puncturing of the material was indicated by a distinct noise. The indenter was then halted from further penetration and gently retracted. This process was repeated for all the manufactured samples. The tested samples were examined through visual inspection and macro-photographs of the fracture zones.

Typical test result data analysis and phases of failure

The data collected by the software included the reactive forces on the indenter by the test sample, measured in Newtons, in relation to the position of the intender, measured in millimetres. The collected data was subsequently normalised based on the thickness of the corresponding sample. The data was normalised to

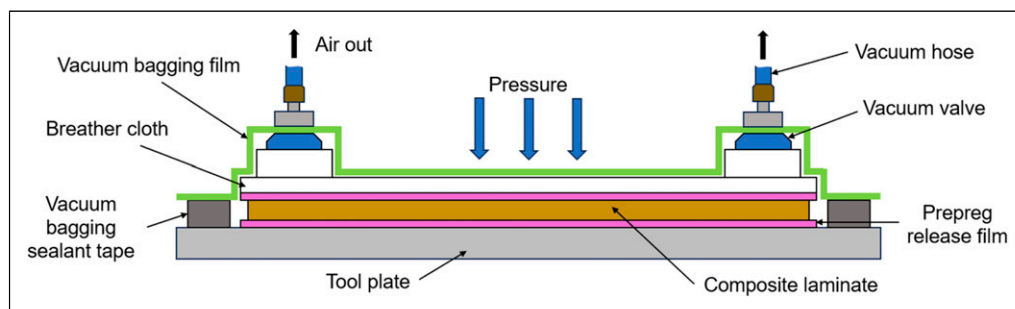


Figure 2. Cross-sectional illustration of laminate bagged and under pressure in the autoclave.

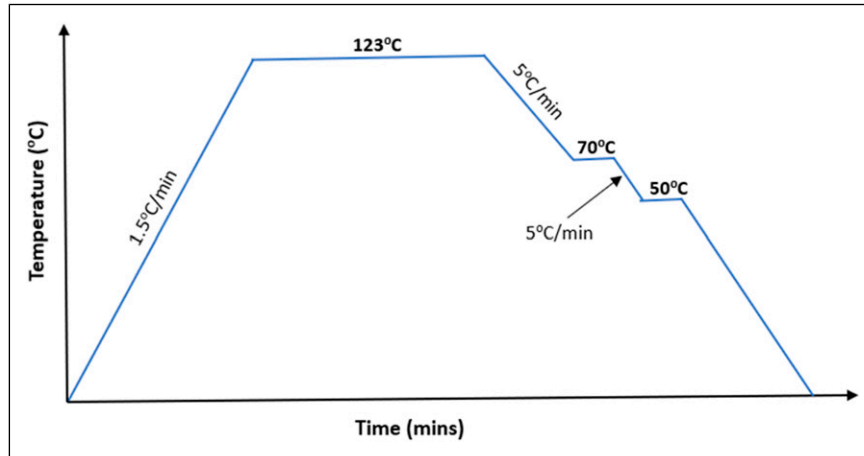


Figure 3. Laminite cure cycle.

facilitate a comparative analysis of the mechanical properties per unit millimetre of the manufactured material. The typical normalised values for force and displacement data plotted on a graph, is illustrated in [Figure 7](#), depicting the phases of the penetration and perforation process that is elastic deformation, damage, and friction.

During the elastic phase, characterised by a linear or near-linear increase in force with displacement, the material is likely to undergo matrix cracking and deformation as the indenter penetrates. As the loading progress the material reaches its maximum load-bearing capacity. Subsequently, in the damage phase, further penetration leads to material fracture and failure. This is often accompanied by fibre rupture and plugging, where fibres obstruct the indenter's path. [Figure 7](#) depicts the different indenter positions. Initially, at position (a), the

indenter closely aligns with the material's surface. As force increases, the indenter bends the material causing some damage likely to be delamination at (b). The indenter penetrates the first layer of the sandwich composite at position (c), where it reaches its ultimate force. The loading on the structure keeps increasing until the indenter fully penetrates the core material at (d), and the lower skin at (e), thereby completing the test phase, where is seen the final drop in the load depicting the friction between the indenter surface and the test material.

Fibre breakage is expected in the second stage of the loading response history and is associated with the sudden load drop. This failure is also accompanied by fibre pull out³⁰ occurring after fibre fracture and is seen as the fibre leaves the matrix if viewed by a cut through the section damage. To quantify the total energy absorbed by the

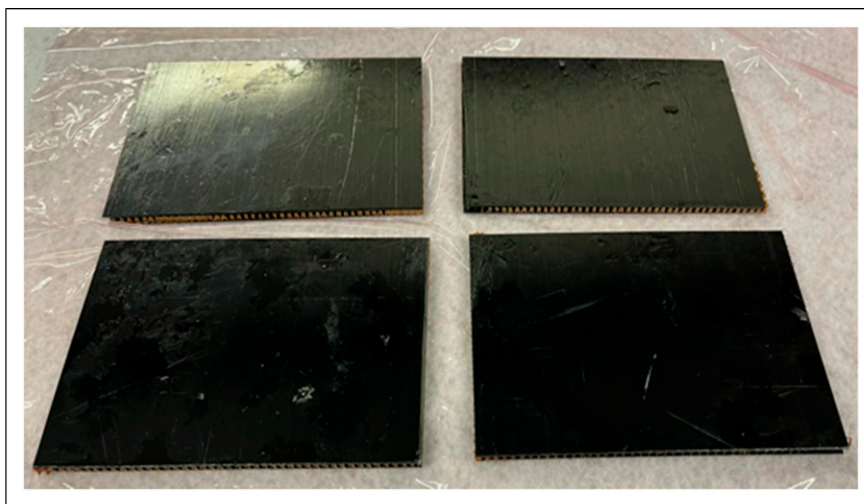


Figure 4. Representative images of sandwich samples manufactured.

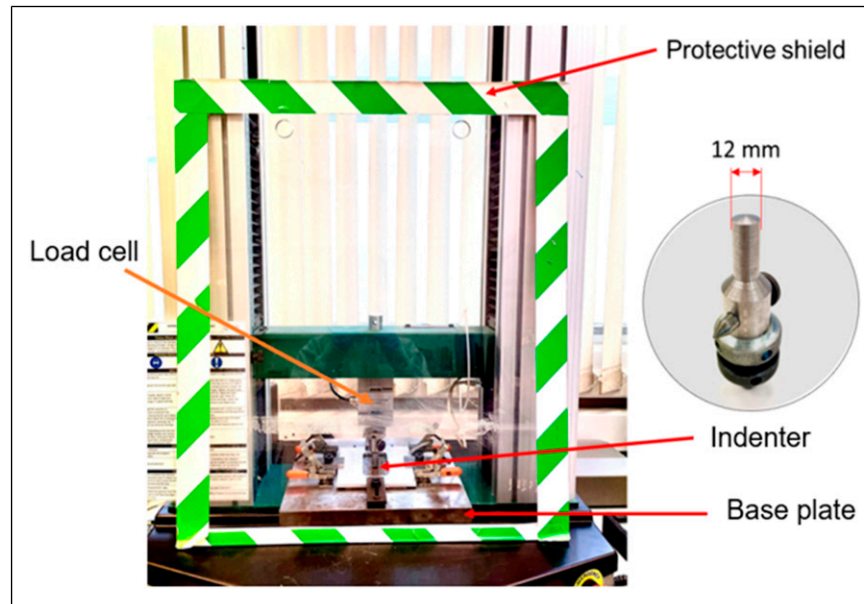


Figure 5. Quasi-static loading test set up.

material up to complete penetration during the loading test, the trapezoidal rule was used to calculate the area under the force-displacement curve.

Experimental results

To investigate the characteristics of the sandwich panel under the low speed loading the sample was clamped round the boundaries and under the indentation load through the central point using the universal testing machine. The movement of the cross head applying the loading was 10 mm/min. The system measures the load – displacement response from the resistive force of the test sample to the loading.

Figures 8–11 shows the load-displacement graphs of the composite plates. It provides insights into the material's stiffness, strength, and failure behaviour under load. The graph typically shows a near linear relationship initially, depicting some elastic behaviour, followed by a nonlinear region as damage evolves the structure and it eventually fails. The plotted data were normalised with the sample thickness for better comparison of the various characteristics. Caprino et al.³¹ highlighted the significance of these curves as they give useful information about the damage phenomenon and the response of the structures.

The load – displacement graphs of the sandwich plates of $[0^\circ/30^\circ/60^\circ/90^\circ]_s$ carbon fibre reinforced skin laminate and core materials of hemp, honeycomb and foam are compared in Figure 8. The response pattern of the three seem to be

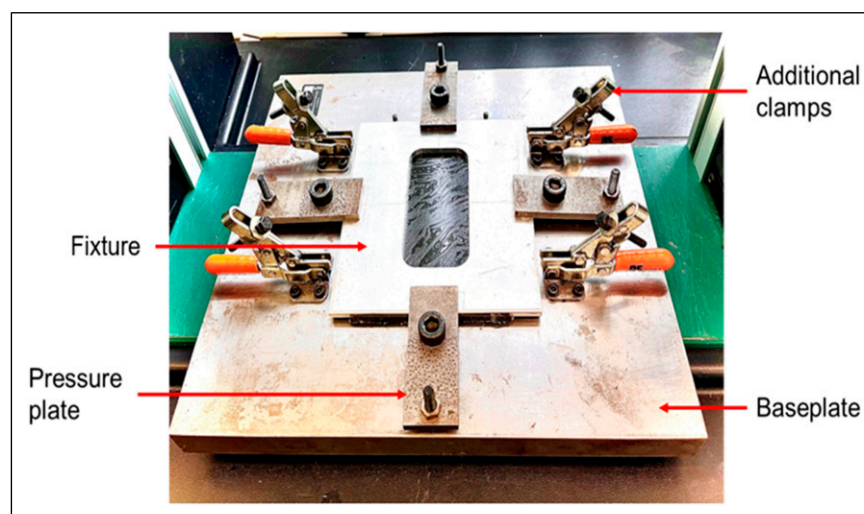


Figure 6. Test rig.

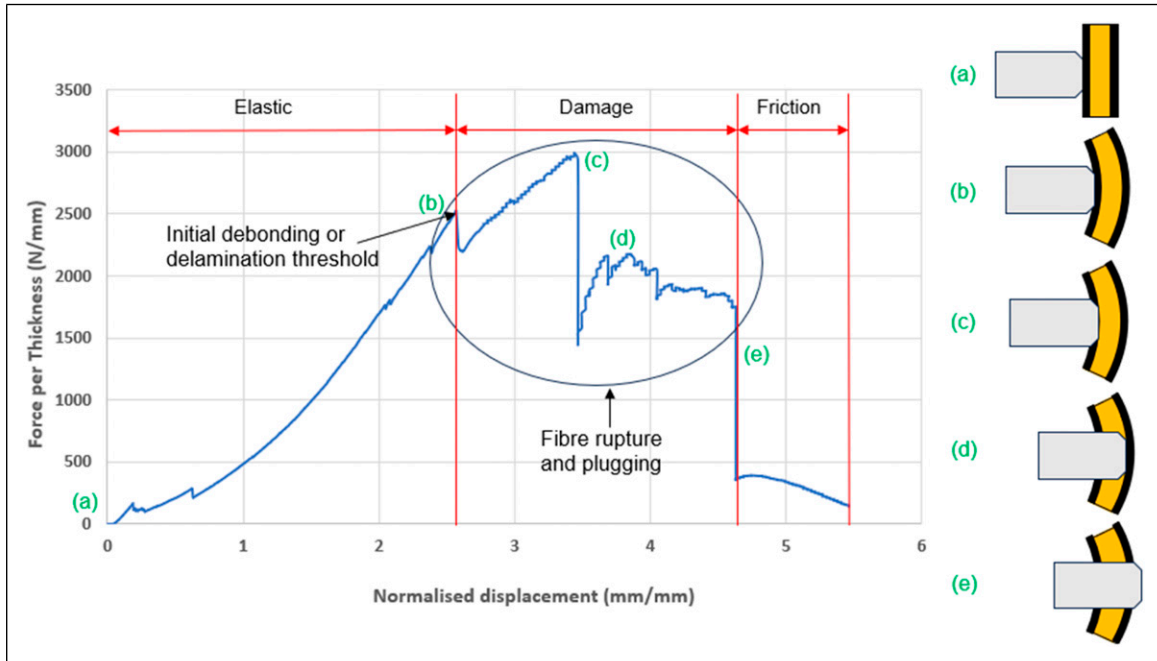


Figure 7. Illustration of force versus displacement graph, with indenter position indicated, for each phase.

similar, this is likely because of the dominance of the skin structure. In all the plot rise to the peak load, but seen after the peak load is the several drops in the load indicating the combination of the various forms damage ie matrix crack, debonding, fibre breakage etc. The average peak loads are

2730 N/mm, 1321 N/mm and 1312 N/mm respectively for the ones with core materials of hemp, honeycomb and foam respectively. The $[0^\circ/30^\circ/60^\circ/90^\circ]_s$ carbon fibre reinforced skin with hemp core endured the highest peak load of 2730 N/mm indicating that it most tolerant to the damages

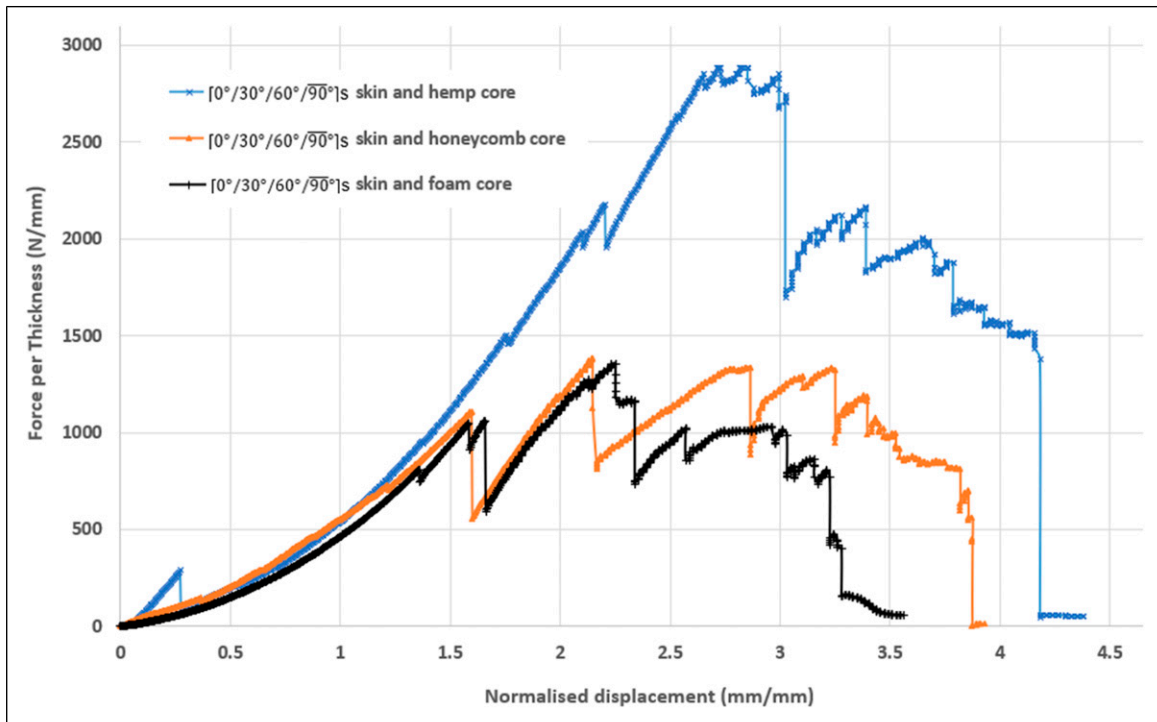


Figure 8. Representative loading response for $[0^\circ/30^\circ/60^\circ/90^\circ]_s$ carbon fibre reinforced skin with various core types of sandwich panels.

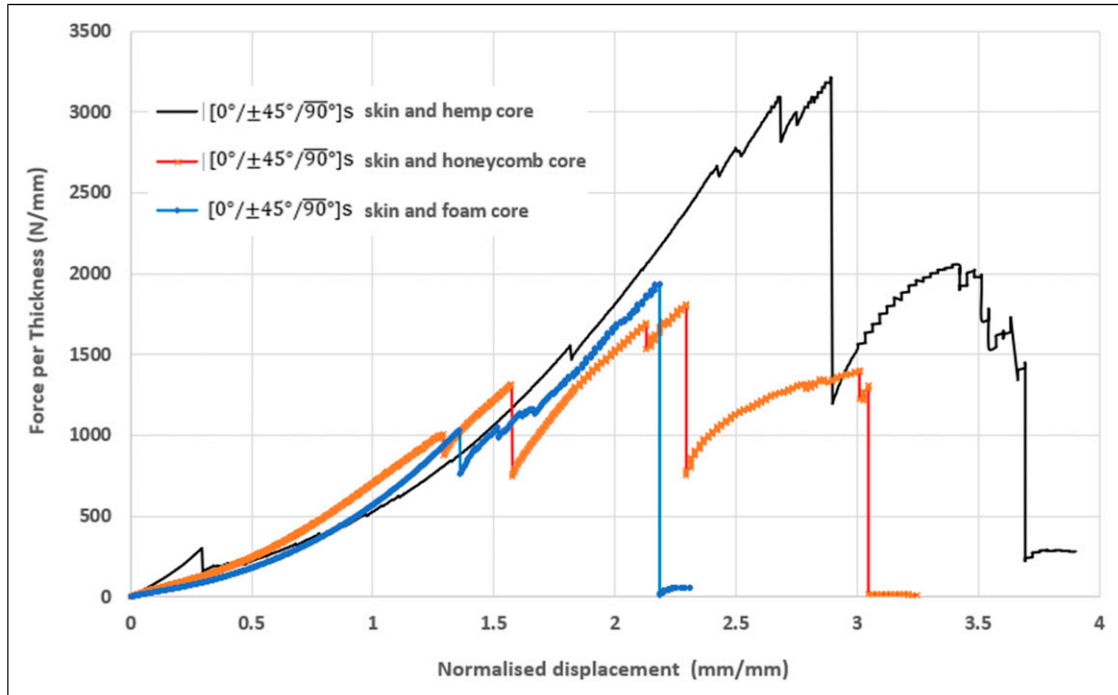


Figure 9. Representative loading response for $[0^\circ/\pm 45^\circ/90^\circ]_s$ carbon fibre reinforced skin with various core types of sandwich panels.

and the spiral nature of the ply stacking sequence is likely to have contributed to the behaviour of all the sandwich plates.

Comparing the response in Figures 8 and 9 shows the difference between the half layup spiral configuration $[0^\circ/30^\circ/60^\circ/90^\circ]_s$ carbon fibre reinforced skin and the quasi-

isotropic layup of $[0^\circ/\pm 45^\circ/90^\circ]_s$. The peak load was higher for the quasi-isotropic laminates; this primarily is because of the $\pm 45^\circ$ plies. The average peak loads are 3238 N/mm, 1557 N/mm and 1635 N/mm respectively for the ones with core materials of hemp, honeycomb and foam

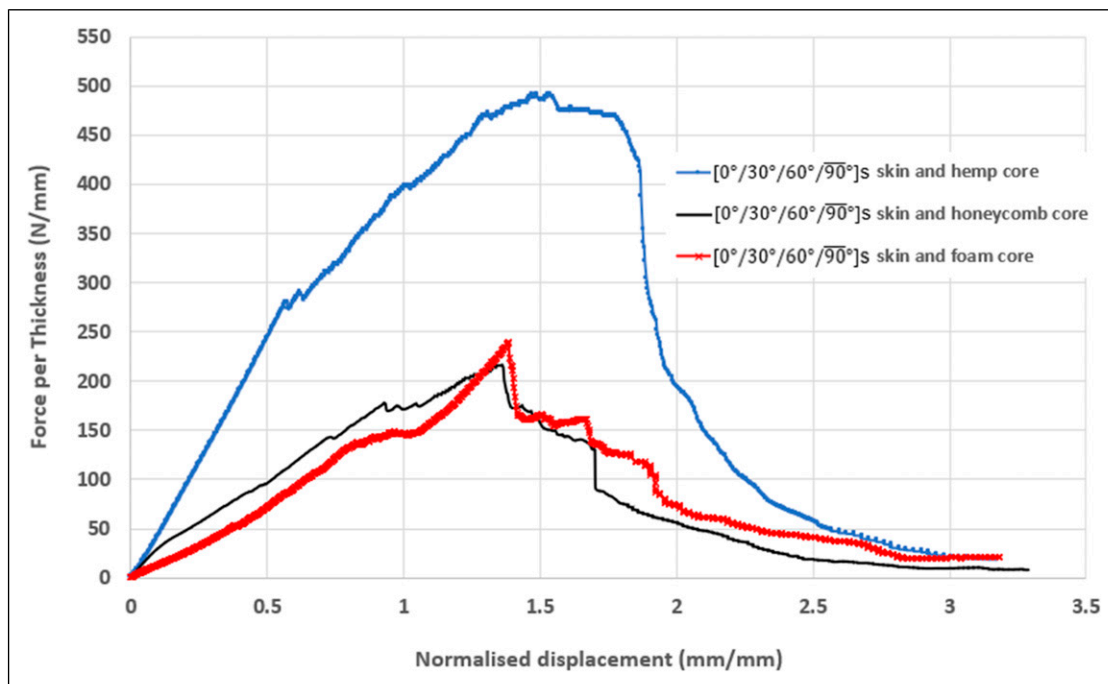


Figure 10. Representative loading response for $[0^\circ/30^\circ/60^\circ/90^\circ]_s$ flax fibre reinforced skin with various core types of sandwich panels.

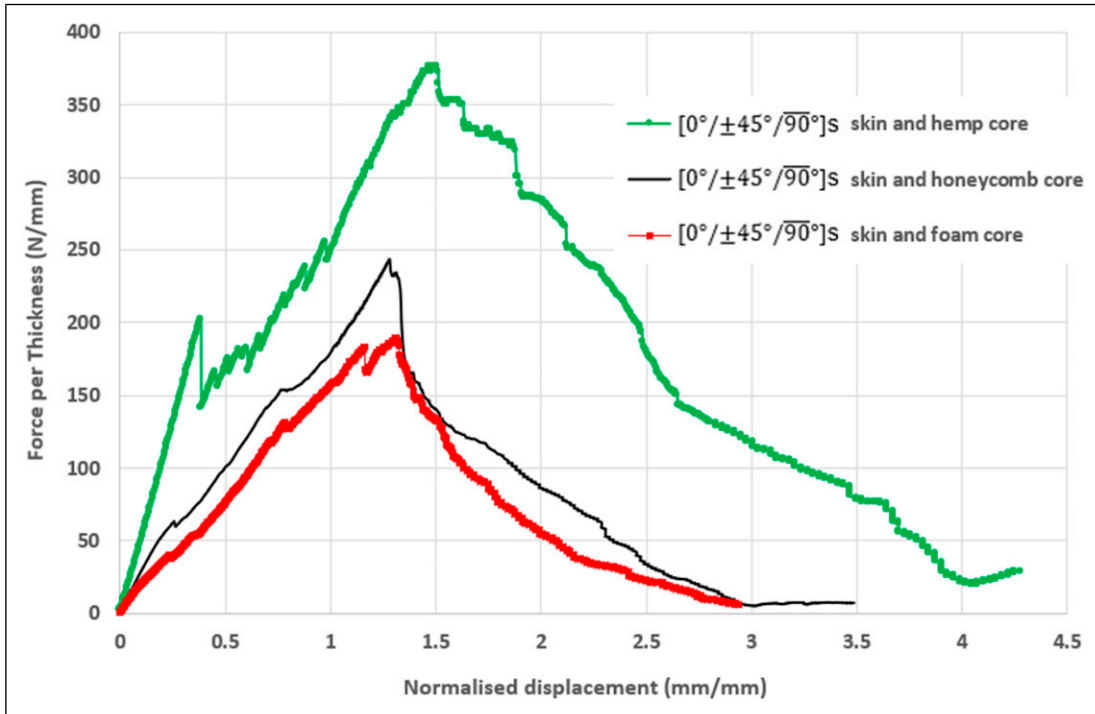


Figure 11. Representative loading response for $[0^\circ/\pm 45^\circ/90^\circ]_s$ flax fibre reinforced skin with various core types of sandwich panels.

and can directly be compared to the spiral skin configuration ones.

The response of the sandwich plates with flax fibre reinforced polymer laminate skins are quite different compared to the ones with carbon fibre as reinforcement on the skin structure as shown in Figures 10 and 11. This is likely because of the relatively better ductility of the natural fibres compared to synthetic ones. Carbon is mainly designed to

withstand high rigidity and strength at the cost of ductility, while the use of natural fibres has the advantage of reducing the environmental impact at end of the life cycle.

In Figures 10 and 11, the graphs rise to some peak value and then gradually drops to zero force value with little or no sharp drop of the loading indicating no major damage in the structure but loss of strength. The characteristics of the plots are of course because the different stacking configurations of

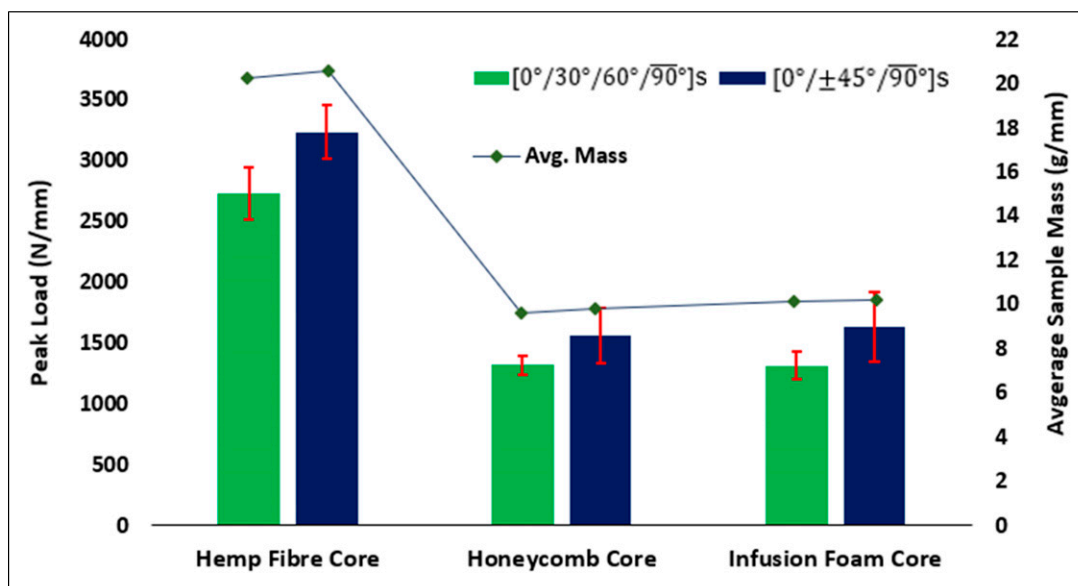


Figure 12. Peak loads observed in sandwich panels with carbon fibre skins.

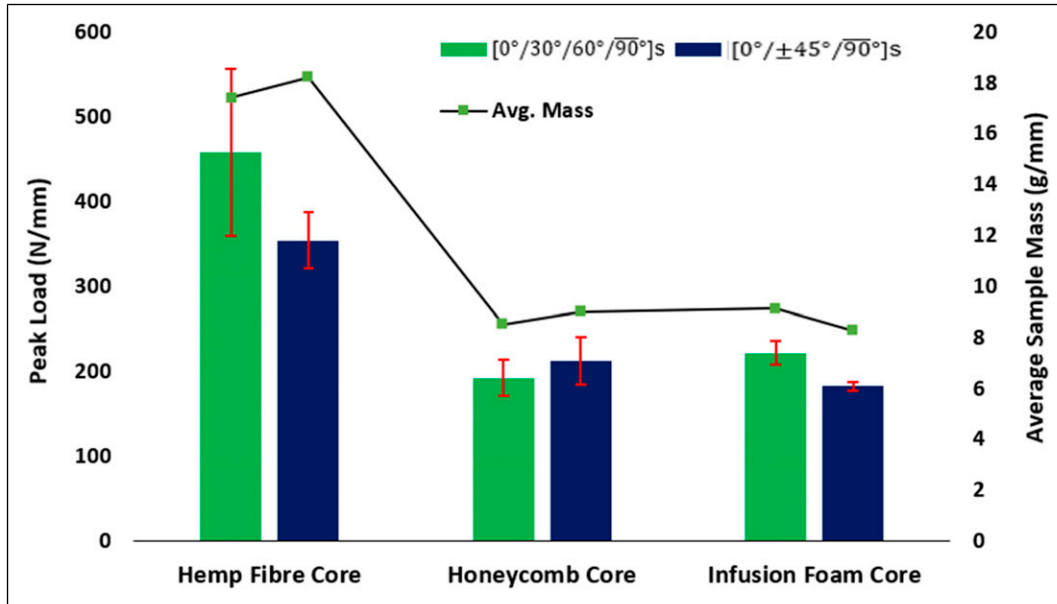


Figure 13. Peak loads observed in sandwich panels with flax fibre skins.

the laminates and the different core materials of the sandwich structure. The average peak loads of $[0^\circ/30^\circ/60^\circ/90^\circ]_s$ flax fibre reinforced skin with hemp as the core as shown in Figure 10 is significantly higher than the ones with foam and aramid paper honeycomb materials. The values are respectively 459 N/mm, 222 N/mm and 193 N/mm this is because of the high strength of hemp (108 MPa) compared to the foam (1.44 MPa) and honeycomb (2.4 MPa) materials as obtained from the data sheet on the manufacturer's website.^{25–27} In Figure 11 is the comparison of the response of the sandwich plate with the quasi-isotropic lay-up and the different core materials. The one with $[0^\circ/\pm 45^\circ/90^\circ]_s$ flax fibre reinforced skin and hemp as core still produced the peak load.

Strength analysis of the structures

The mean values for peak loads and energy absorption determined from force-displacement curves of sandwich composites were plotted in a bar chart. In addition to displaying mean values, the graphs also present the error bars of four repeat test per sample indicating the standard deviations (Figures 12 and 13).

Table 6. The peak loads values from the sandwich panels with carbon fibre skins.

Core material	$[0^\circ/30^\circ/60^\circ/90^\circ]_s$	$[0^\circ/\pm 45^\circ/90^\circ]_s$
Hemp fibre	2730.2 ± 216.1 (N/mm)	3237.7 ± 223.1 (N/mm)
Honeycomb	1321.3 ± 77.1 (N/mm)	1557.2 ± 226.5 (N/mm)
Infusion foam	1312.1 ± 113.8 (N/mm)	1635.5 ± 284.7 (N/mm)

The peak loads for sandwich panels with carbon fibre skins with the average sample mass are plotted in Figure 12 and the values of the peak loads shown in Table 6. The calculated specific peak loads from the test data are shown in Table 7 it is the peak load per unit mass. It was evident that panels featuring $\pm 45^\circ$ skins exhibited superior load-bearing capacity across all core materials compared to those with combined 30° and 60° skins. This could be because carbon fibre skins with unidirectional plies in $\pm 45^\circ$ angles distribute load more effectively as opposed to those with 30° and 60° fibre orientations. Additionally, sandwich composites incorporating a hemp fibre core demonstrated the ability to endure approximately twice the loading on the panels compared to the other core materials.

In Figure 13 is shown the ultimate forces endurable by the sandwich panels with flax fibre as reinforcement of the skin laminate structure, along with their average mass and the values of the peak loads shown in Table 8. Presented in Table 9 are the calculated specific peak load values. In contrast to carbon fibre reinforced laminate skin sandwich composites, flax fibre skins laminate sandwich with 30° and 60° angle plies demonstrates enhanced load-bearing capacities in comparison to the $\pm 45^\circ$ fibre orientation, when combined with hemp fibre and infusion foam core. The highest peak of about 459 N/mm was produced

Table 7. Specific peak loads in the carbon fibre skin structures.

Core material	$[0^\circ/30^\circ/60^\circ/90^\circ]_s$	$[0^\circ/\pm 45^\circ/90^\circ]_s$
Hemp fibre	134.7 ± 10.7 (N/g)	157.6 ± 10.9 (N/g)
Honeycomb	137.5 ± 8.0 (N/g)	158.9 ± 23.1 (N/g)
Infusion foam	129.4 ± 11.2 (N/g)	160.5 ± 27.9 (N/g)

Table 8. The peak loads values from the sandwich panels with flax fibre skins.

Core material	$[0^\circ/30^\circ/60^\circ/90^\circ]_s$	$[0^\circ/\pm 45^\circ/90^\circ]_s$
Hemp fibre	458.7 ± 98.1 (N/mm)	354.7 ± 33.4 (N/mm)
Honeycomb	192.9 ± 21.6 (N/mm)	212.6 ± 28.0 (N/mm)
Infusion foam	222.5 ± 13.7 (N/mm)	182.8 ± 5.2 (N/mm)

by the $[0^\circ/30^\circ/60^\circ/90^\circ]_s$ skin with hemp as the core material as shown in Figure 13 this is likely because of the fibre's configuration, the affinity between the two natural materials and the strength properties of hemp compared to the foam and Nomex paper honeycomb structures. De Fazio et al.³² reported about the potential of hemp for high-performance sandwich cores structures. In general, the properties depend on chemical composition and structure, which are influenced by factors including fibre type, growing conditions, harvesting time, extraction method, treatment, and storage procedures³³.

Comparison of the energy absorption

The data obtained from the quasi-static loading test on the samples were plotted as force-displacement curve and the area under these graphs were estimated using trapezoidal approach, which represents the work done by the indenter on the samples. This is equivalent to the energy absorbed and dissipated by the samples.

Figure 14 presents the data for the energy absorbed by samples with carbon fibres as reinforcement in the skin structures and the values of the absorbed energy shown in Table 10. Specific energy absorbed data known as the energy absorbed/dissipated per unit mass of structures are presented in Table 11. The structure with hemp as the core and $[0^\circ/30^\circ/60^\circ/90^\circ]_s$ made of carbon as reinforcement absorbed more energy compared to the $\pm 45^\circ$ skin variant. Similar characteristics of results were seen for the samples with infusion foam core materials. Surprisingly, based on the mean results of the four test the trend was seen to be reversed for the honeycomb core material, but considering the upper boundaries of the error bars the original trend still stands. These results conclude that the cyclic trend of the $[0^\circ/30^\circ/60^\circ/90^\circ]_s$ configuration can absorb more energy than the $[0^\circ/\pm 45^\circ/90^\circ]_s$ laminate.

In Figure 15, the energy absorbed by samples with flax fibre as reinforcement of the skins is illustrated and the energy

Table 9. Specific peak loads in the flax fibre skin structures.

Core material	$[0^\circ/30^\circ/60^\circ/90^\circ]_s$	$[0^\circ/\pm 45^\circ/90^\circ]_s$
Hemp fibre	26.3 ± 5.6 (N/g)	19.5 ± 1.8 (N/g)
Honeycomb	22.6 ± 2.5 (N/g)	23.6 ± 3.1 (N/g)
Infusion foam	24.3 ± 1.5 (N/g)	22.1 ± 0.6 (N/g)

Table 10. Energy absorbed values from the sandwich panels with carbon fibre skins.

Core material	$[0^\circ/30^\circ/60^\circ/90^\circ]_s$	$[0^\circ/\pm 45^\circ/90^\circ]_s$
Hemp fibre	6012.4 ± 32.0 (J/mm)	4788.0 ± 714.1 (J/mm)
Honeycomb	2040.7 ± 885.0 (J/mm)	2635.6 ± 229.3 (J/mm)
Infusion foam	2215.1 ± 326.1 (J/mm)	1622.7 ± 326.1 (J/mm)

absorbed values presented in Table 12; also shown the Table 13 are the specific energy absorption data. A notable difference was observed between the energy absorbed values for flax fibre reinforced epoxy laminate skins with hemp fibre and those with other core materials. The energy absorbed by the flax fibre skin samples with foam and honeycomb core followed a different trend compared to the other one. The difference in the mean value of the energy absorbed is small [24 J/mm] for the honeycomb core sandwich samples.

Examination of failure modes

Understanding the modes of failure will help in the optimisation of the composite design and drive innovation with the applications. Figure 16 show cases different failure modes observed in the cross-sectional view of the damage region of the sandwich panels. Predominantly, samples of stacking sequence $[0^\circ/30^\circ/60^\circ/90^\circ]_s$ made of carbon/epoxy plies skins exhibited delamination and fibre breakage, indicating the brittle nature of carbon fibres. Furthermore, core crushing was evident in the samples with honeycomb and infusion foam cores. This occurred as the load applied on the samples exceeded the compressive strength of the mentioned core materials. In contrast, sandwich panels with hemp fibre core exhibited matrix cracking and fibre damage like that observed in the carbon fibre skins, thereby avoiding the occurrence of core crushing. The damage modes in loaded composite laminates are often interrelated; matrix cracking can initiate delamination, and fibre breakage can occur due to the failure of the matrix. The design of composite laminates seeks to optimise the fibre orientations to mitigate the damage mechanisms.

When a composite is loaded on a surface the resulting damage on the structure varies depending on the configuration, material type and the loading energy. This usually result to the front surface showing dents or indentations and matrix cracking. The indenter compresses the surface,

Table 11. Specific energy absorption in the carbon fibre skin structures.

Core material	$[0^\circ/30^\circ/60^\circ/90^\circ]_s$	$[0^\circ/\pm 45^\circ/90^\circ]_s$
Hemp fibre	296.7 ± 1.6 (J/g)	233.1 ± 34.8 (J/g)
Honeycomb	212.4 ± 92.1 (J/g)	268.9 ± 23.4 (J/g)
Infusion foam	218.5 ± 32.2 (J/g)	159.3 ± 32.0 (J/g)

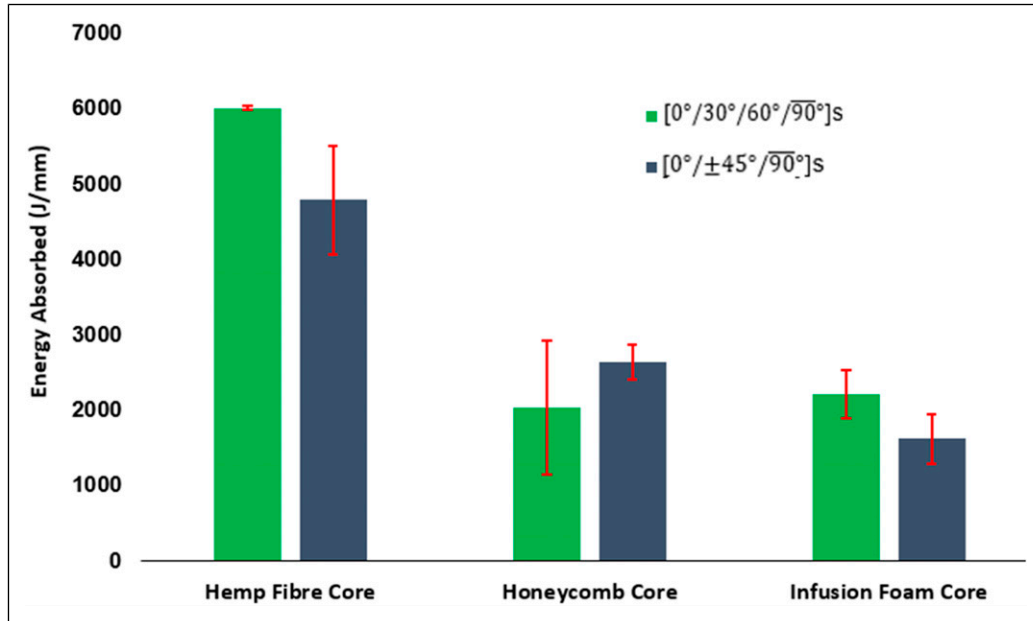


Figure 14. Energy absorbed by sandwich panels with carbon fibre skins normalised with the sample thickness.

cracking the matrix and breaking some of the fibres. In Figures 17 and 18 is illustrated the various failure modes on the rear surfaces of the tested sandwich structures. The rear surfaces are usually in tension due to the loading and failure modes shown include fibre breakage, fibre peel-out and matrix crack. Matrix cracking is one of the damages induced during quasi static loading and it is because to high stresses at the location of loading.³⁴ Comparing the rear surface damage characteristics of the sandwich plates with carbon fibre reinforce laminate skin in Figure 17 and the ones with

flax fibre as reinforcement shown in Figure 18 the later was more localised. This is thought to be because of the strength carbon fibre, which is much higher than flax fibre.

Debonding between core materials and skins was a common occurrence across all samples. The primary mode of failure for the samples with [0°/±45°/90°]s carbon fibre/epoxy skin was delamination and fibre breakage. Unlike the carbon fibre skins, the delamination of flax fibre skins panels occurs in more contained sections, with fibres pulling out in groups rather than individually. This results in fewer

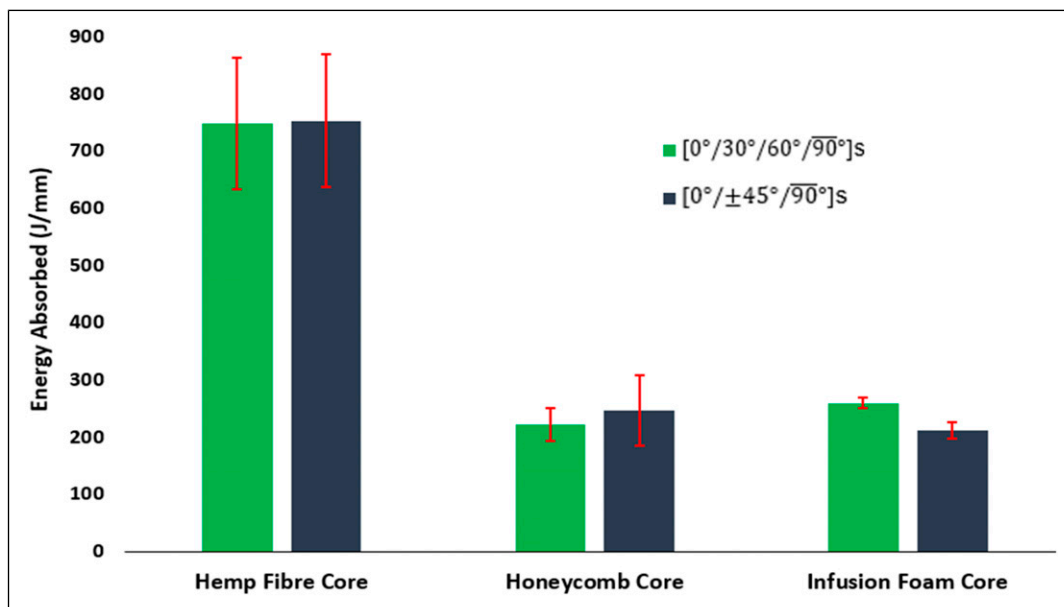


Figure 15. Energy absorbed by sandwich panels with flax fibre skins normalised with the sample thickness.

Table 12. Energy absorbed values from the sandwich panels with flax fibre skins.

Core material	$[0^\circ/30^\circ/60^\circ/90^\circ]_s$	$[0^\circ/\pm 45^\circ/90^\circ]_s$
Hemp fibre	748.4 ± 114.9 (J/mm)	753.1 ± 116.0 (J/mm)
Honeycomb	222.7 ± 28.3 (J/mm)	247.0 ± 61.7 (J/mm)
Infusion foam	259.8 ± 8.9 (J/mm)	212.6 ± 14.0 (J/mm)

Table 13. Specific energy absorption in the flax fibre skin structures.

Core material	$[0^\circ/30^\circ/60^\circ/90^\circ]_s$	$[0^\circ/\pm 45^\circ/90^\circ]_s$
Hemp fibre	42.9 ± 6.6 (J/g)	41.3 ± 6.4 (J/g)
Honeycomb	26.1 ± 3.3 (J/g)	27.4 ± 6.8 (J/g)
Infusion foam	28.4 ± 1.0 (J/g)	25.7 ± 1.7 (J/g)

**Figure 16.** Cross section view photographs of the damages in the tested samples.

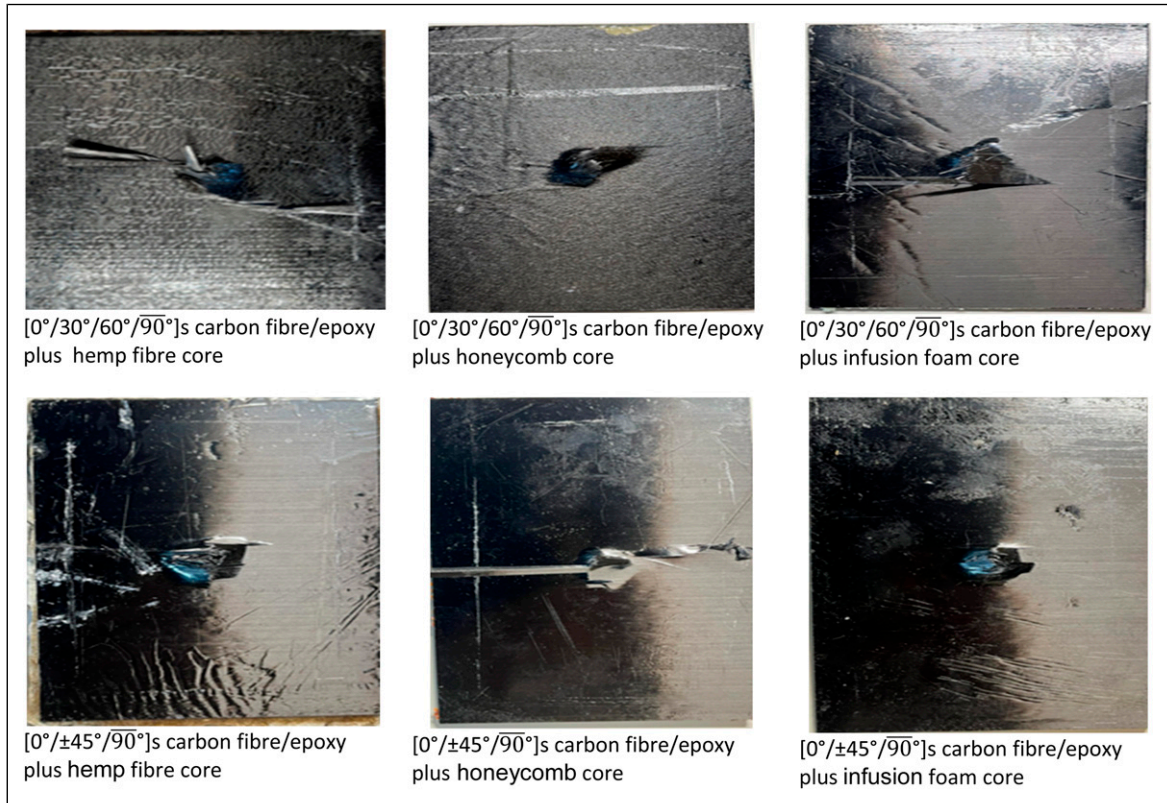


Figure 17. Rear surface damages of samples with carbon fibre reinforcement as the skin structure.

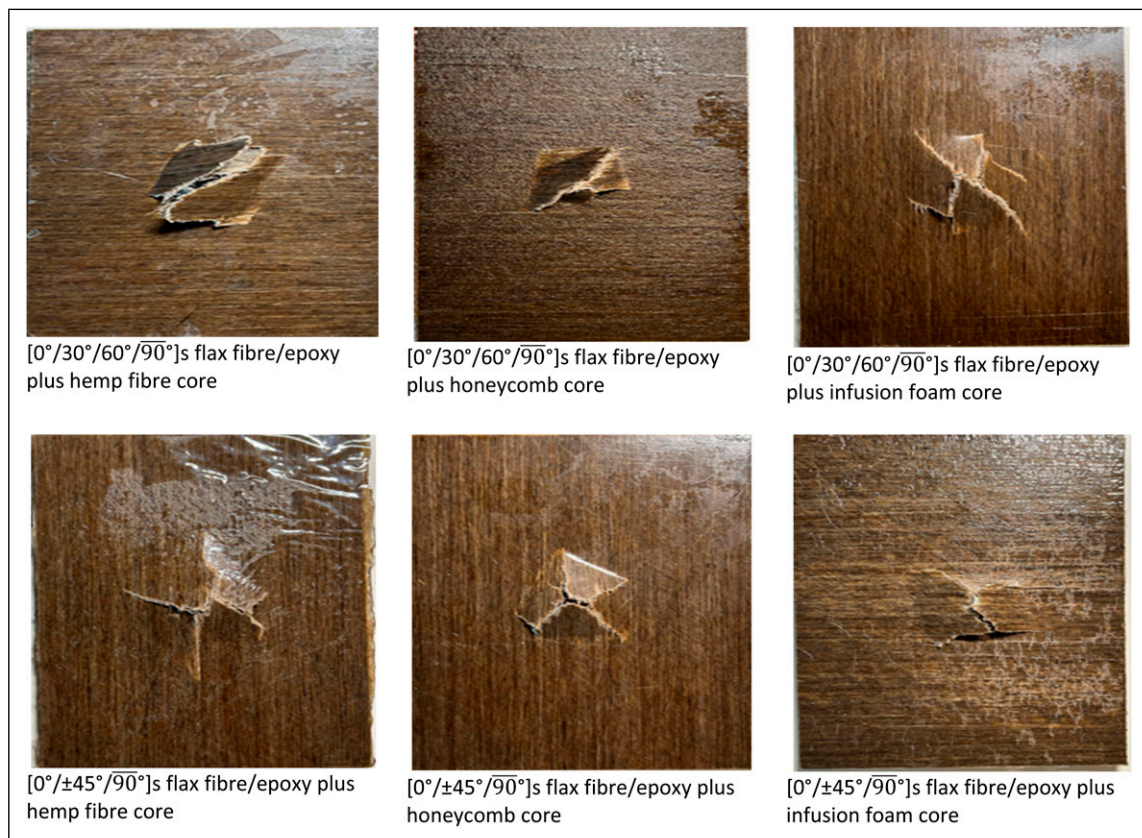


Figure 18. Rear surface damages of samples with flax fibre reinforcement as the skin structure.

particles being dispersed, which is beneficial for recyclability. Debonding between skins and core materials was also observed in these samples.

While carbon fibre reinforced composites are brittle and linear elastic to failure, and this is depicted by the load – displacements graphs from the panels in Figures 8 and 9 by the sharp drops in the load. The panels with the skin reinforced with flax fibres shows gradual loss of the load from the peak to final failure (Figures 10 and 11). This distinction is evident in Figures 17 and 18 where the failure modes of the rear surfaces are illustrated.

Conclusion

The selection of materials, layup configuration, load path and stress distribution help engineers to optimise the structural design of the multi-layered panels for specific applications. With the purpose to contribute to development of sustainable structures, in this work sandwich composites with some percentages of biodegradable materials were manufactured and tested. These samples were tested under quasi-static loading to understand the behaviour of structures under slowly progressing load. The peak load and energy absorbed were estimated from the test data. Additionally, the tested samples were halved through the damage region, and the failure modes were observed.

Following the analysis of the test results, it was evident that the mechanical properties of composite sandwich panels largely depend on the characteristics of the reinforcement fibre being used for the skin laminates, stacking sequence of the laminate, choice of core material, and adhesion between the two. The mechanical properties of the samples featuring carbon fibre skins demonstrated superior characteristics such as the maximum load-bearing capacity and energy absorption compared to samples with flax fibre skins. The following inference was drawn from the results.

- Different core materials exhibit distinct performance characteristics depending on the stacking sequence of the skin with which they are paired. For instance, honeycomb core demonstrated superior performance when paired with flax fibre skin in the stacking orientation $[0^\circ/\pm 45^\circ/\overline{90^\circ}]_s$, whereas foam core exhibited better performance when combined with flax fibre skin featuring a $[0^\circ/30^\circ/60^\circ/\overline{90^\circ}]_s$ fibre orientation, hence this spiral arrangement is a recommendation to consider to improve the damage resistance for light airless core materials sandwich structures.
- Composite samples incorporating hemp fibre core demonstrated better performance across all samples when compared to those with other tested core materials.
- It was evident that honeycomb and foam cores exhibited relatively better performance when paired with carbon fibre skins compared to flax fibre skins.
- The samples incorporating honeycomb and foam core exhibited similar mechanical properties, indicating that either option could be utilised depending on the specific application requirements. However, it's worth noting that samples with foam core tend to be slightly heavier than those with Nomex honeycomb core.
- Delamination and fibre breakage emerged as the primary failure modes across all samples, with flax fibre samples exhibiting fibres pulling out in groups, in contrast to the individual pulling observed in carbon fibre samples.
- Core crushing was observed in samples with honeycomb and foam cores.

Notably, the structures with flax fibres reinforced skin having 30° and 60° angle plies demonstrated good load bearing strength compared to the ones with $\pm 45^\circ$ fibre orientation, this could be because of the spiral nature of the arrangement in the former.

Acknowledgements

The authors would like to acknowledge the University of Hertfordshire, which supported this study.

ORCID iD

Opukuro David-West  <https://orcid.org/0000-0003-3999-9686>

Funding

The authors disclosed receipt of the following financial support for the research, authorship, and/or publication of this article: This work was supported by the University of Hertfordshire.

Declaration of conflicting interests

The authors declared no potential conflicts of interest with respect to the research, authorship, and/or publication of this article.

Data Availability Statement

The raw and processed data that support the findings of this study are available from the corresponding author upon reasonable request.

References

1. Soni R, Verma R, Garg RK, et al. A critical review of recent advances in the aerospace materials. *Mater Today Proc* 2023; 113: 180–184.
2. Kesarwani S. Polymer composites in aviation sector. *Int J Eng Res* 2017; V6(06): 2.
3. Sadeghian P, Hristozov D and Wroblewski L. Experimental and analytical behavior of sandwich composite beams: comparison of natural and synthetic materials. *J Sandw Struct Mater* 2018; 20(3): 287–307.
4. Islam MM and Aravinthan T. Behaviour of structural fibre composite sandwich panels under point load and uniformly distributed load. *Compos Struct* 2010; 93: 206–215.

5. Malcom AJ, Aronson MT, Deshpande VS, et al. Compressive response of glass fiber composite sandwich structures. *Compos A Appl Sci Manuf* 2013; 54: 88–97.
6. Jin F, Chen H, Zhao L, et al. Failure mechanisms of sandwich composites with orthotropic integrated woven corrugated cores: experiments. *Compos Struct* 2013; 98: 53–58.
7. Zhang J, Supernak P, Mueller-Alander S, et al. Improving the bending strength and energy absorption of corrugated sandwich composite structure. *Mater Des* 2013; 52: 767–773.
8. Hou S, Shu C, Zhao S, et al. Experimental and numerical studies on multi-layered corrugated sandwich panels under crushing loading. *Compos Struct* 2015; 126: 371–385.
9. Ruan D, Lu G and Wong YC. Quasi-static indentation tests on aluminium foam sandwich panels. *Compos Struct* 2010; 92: 2039–2046.
10. Farrokhhabadi A, Ahmad Taghizadeh S, Madadi H, et al. Experimental and numerical analysis of novel multi-layer sandwich panels under three point bending load. *Compos Struct* 2020; 250: 112631.
11. Sayahlatifi S, Rahimi GH and Bokaei A. The quasi-static behavior of hybrid corrugated composite/balsa core sandwich structures in four-point bending: experimental study and numerical simulation. *Eng Struct* 2020; 210: 110361.
12. Zarei Mahmoudabadi M and Sadighi M. Experimental investigation on the energy absorption characteristics of honeycomb sandwich panels under quasi-static punch loading. *Aero Sci Technol* 2019; 88: 273–286.
13. Fan H, Zhou Q, Yang W, et al. An experiment study on the failure mechanisms of woven textile sandwich panels under quasi-static loading. *Compos B Eng* 2010; 41: 686–692.
14. Jackson M and Shukla A. Performance of sandwich composites subjected to sequential impact and air blast loading. *Compos B Eng* 2011; 42: 155–166.
15. Chen Y, Hou S, Fu K, et al. Low-velocity impact response of composite sandwich structures: modelling and experiment. *Compos Struct* 2017; 168: 322–334.
16. Zhang W, Qin Q, Li J, et al. Deformation and failure of hybrid composite sandwich beams with a metal foam core under quasi-static load and low-velocity impact. *Compos Struct* 2020; 242: 112175.
17. Hachemane B, Zitoune R, Bezzazi B, et al. Sandwich composites impact and indentation behaviour study. *Compos B Eng* 2013; 51: 1–10.
18. Zhao Y, Yan S and Jia J. Fabrication and statics performance of pyramidal lattice stitched foam sandwich composites. *Comput Model Eng Sci* 2021; 126(3): 1251–1274.
19. Mazzuca P. Flexural behaviour of GFRP sandwich panels with eco-friendly PET foam core for the rehabilitation of building floors. *Structures* 2024; 60: 105815.
20. Abdel-Nasser Y, Elhewy AMH and Al-Mallah I. Impact analysis of composite laminate using finite element method. *Ships Offshore Struct* 2016; 12: 219–226.
21. Mahboob Z, El Sawi I, Zdero R, et al. Tensile and compressive damaged response in flax fibre reinforced epoxy composites. *Compos A Appl Sci Manuf* 2017; 92: 118–133.
22. Benedict LS, Fawaz Z and Bougherara H. Numerical simulation correlating the low velocity impact behaviour of flax/epoxy laminates. *Compos A Appl Sci Manuf* 2019; 126: 105582.
23. Gumanová V, Sobotová L, Dzuro T, et al. Experimental survey of the sound absorption performance of natural fibres in comparison with conventional insulating materials. *Sustainability* 2022; 14: 4258.
24. Etaati A, Mehdizadeh SA, Wang H, et al. Vibration damping characteristics of short hemp fibre thermoplastic composites. *J Reinforc Plast Compos* 2014; 33(4): 330–341.
25. 150g non-woven hemp fibre mat (480mm) (easy composites) data sheet. <https://www.easycomposites.co.uk/150g-non-woven-hemp-fibre-mat> (accessed 7th September 2025).
26. 3DCORE PET 100 infusion foam manufacturer (easy composites) data sheet. <https://www.easycomposites.co.uk/3d-core-infusion-foam-core> (accessed 7th September 2025).
27. 3.2mm cell 29kg Nomex aerospace honeycomb, (easy composites) data sheet. <https://www.easycomposites.co.uk/3mm-29kg-aerospace-nomex-honeycomb>, (accessed 11th September 2025).
28. ASTM D7136/D7136M-12. *standard test method for measuring the damage resistance of a fibre-reinforced polymer matrix composite to a drop-weight impact event*, 2015.
29. Krzyżak A, Mazur M, Gajewski M, et al. Sandwich structured composites for aeronautics: methods of manufacturing affecting some mechanical properties. *Int J Aerosp Eng* 2016; 2016: 1–10.
30. Siddiqui MAS, Rabbi MS and Dewanjee S. Low-velocity impact response of natural fiber reinforced composites: a comprehensive review on influential parameters. *Compos C Open Access* 2023; 12: 100422.
31. Caprino G, Lopresto V, Scarponi C, et al. Influence of material thickness on the response of graphite fabric/epoxy panels to low velocity impact. *Compos Sci Technol* 1999; 59/15: 2279–2286.
32. De Fazio D, Boccarusso L, Cuomo S, et al. Impact behaviour of a new hemp/carbon sandwich structure. *Proced CIRP* 2021; 99: 432–436.
33. Pickering KL, Efendy MGA and Le TM. A review of recent developments in natural fibre composites and their mechanical performance. *Compos A Appl Sci Manuf* 2016; 83: 98–112.
34. Wan L, Ismail Y, Sheng Y, et al. A review on micromechanical modelling of progressive failure in unidirectional fibre-reinforced composites. *Compos C Open Access* 2023; 10: 100348.